

Earthquake-induced settlement analysis for rockfill dams using cumulative damage theory

Y. Yamaguchi, H. Satoh & K. Shimoyama

Dam Structure Team, Public Works Research Institute (PWRI), Tsukuba, Japan

ABSTRACT: According to “Guidelines for Seismic Safety Evaluation of Dams (Draft)” in Japan, the seismic safety of rockfill dam is basically evaluated based on the sliding deformation due to large earthquake motion. But, during the Niigata-ken Chuetsu Earthquake in 2004, relatively large settlements without sliding were observed at rockfill dams at which consolidation settlement thought to have almost finished before the earthquake. Thus, to accurately estimate the settlement due to large earthquake motions, the settlement should be reproduced by other methods, such as deformation analysis based on cumulative damage theory. We clarify the dynamic strength of construction materials for rockfill dams from the results of cyclic triaxial tests under various conditions, and execute earthquake-induced deformation analysis.

We conduct dynamic laboratory tests for construction materials and evaluate differences of dynamic properties due to the confining pressure and the saturated/unsaturated conditions. We calculate settlements induced by large earthquake motions using cumulative damage theory and evaluate differences due to the confining pressure and saturated/unsaturated conditions. We find that it is very important for accurate evaluation of earthquake-induced settlement to use the laboratory test results considering confining pressure and saturated/unsaturated conditions.

1 INTRODUCTION

In the “Guidelines for Seismic Safety Evaluation of Dams (Draft)” issued by the River Bureau of the Ministry of Land, Infrastructure, Transport and Tourism in March, 2005 (MLIT, 2005), seismic performance of embankment dams is basically evaluated based on sliding deformation. This evaluation method stands on technical and empirical judgments that earthquake-induced settlement without accompanying sliding formation due to a large earthquake motion is about equal to future consolidation settlement (JDEC, 2001) and that earthquake-induced settlement is smaller than the settlement by sliding deformation. Nevertheless, post surveys of rockfill dams that had been damaged in the Niigata-ken Chuetsu Earthquake in 2004 revealed that relatively large-scale settlements occurred without sliding deformation (JR East Co., 2006). So, we should investigate other evaluation methods such as cumulative damage theory analysis (hereafter, CDTA) in addition to the sliding deformation analysis to accurately evaluate earthquake-induced settlement of rockfill dams due to large earthquake motions.

In this study, dynamic strength tests for construction materials were conducted under various conditions in terms of confining pressure and saturated/unsaturated conditions and the previous test results were reviewed to evaluate the effects of those conditions on the dynamic strength. Furthermore, we calculated earthquake-induced settlements by CDTA using the dynamic strength properties in order to examine the effects of the confining pressure and saturated/unsaturated conditions.

2 EFFECTS OF CONFINING PRESSURE AND SATURATED/UNSATURATED CONDITIONS ON DYNAMIC STRENGTH

When a rockfill dam is constructed and impounded, there are saturated/unsaturated areas in dam body and the confining pressure distribution in the dam body varies according to the depth from the surface. The dynamic strength properties of rockfill dam materials can be assumed to be subject to such factors as confining pressure and saturated/unsaturated conditions.

In this chapter, we review the previous test results of dynamic strength tests for rockfill dam materials under various conditions regarding confining pressure and saturated/unsaturated conditions and evaluate the effects of those conditions on dynamic strength properties. Further, we carry out dynamic strength tests in saturated/unsaturated conditions using rock materials of a rockfill dam that is currently under construction.

2.1 Effects of confining pressure

Matsumoto *et al.* (Matsumoto, 1991) conducted cyclic triaxial tests on the rock materials of the Sagurigawa Dam by applying several levels of mean effective stress, σ'_m . Figure 1 illustrates the cumulative strain for each σ'_m value. As the value of σ'_m becomes smaller, the shear stress ratio that generates the same level of strain in the same number of cycles increases. This indicates that dynamic strength increases as the confining pressure decreases.

2.2 Effects of saturated/unsaturated conditions

Satoh and Yamaguchi (Satoh, 2007) conducted cyclic triaxial tests in saturated/unsaturated conditions on the core materials of Dam A (an earth core rockfill dam (ECRD)), which is currently under construction. Figure 2 illustrates the cumulative strain in saturated/

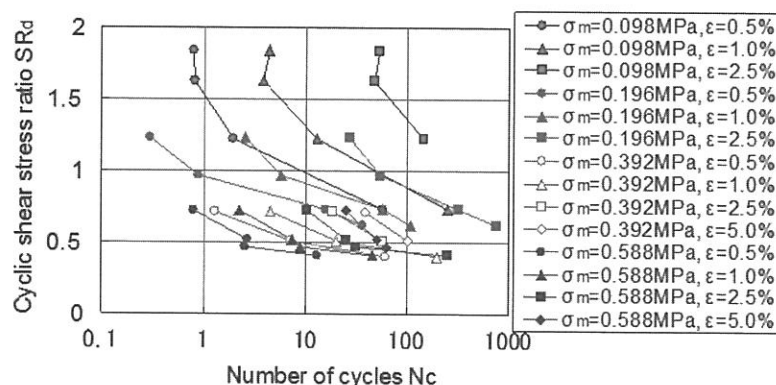


Figure 1. Cumulative strain of the rock materials of the Sagurigawa Dam by cyclic loading.

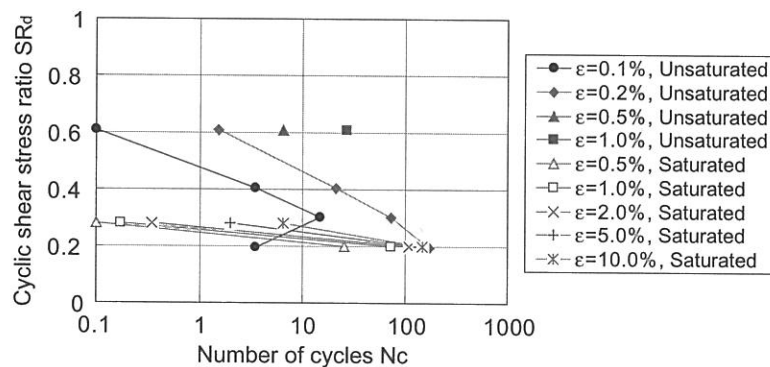


Figure 2. Cumulative strain properties of the core materials of Dam A.

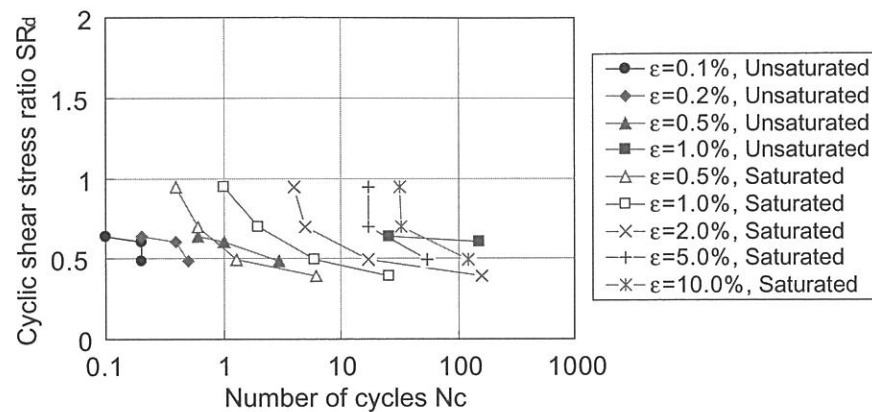


Figure 3. Cumulative strain of the rock materials of Dam A.

unsaturated conditions and indicates that the dynamic strength in unsaturated condition is larger than that in saturated condition.

2.3 Dynamic strength tests on rock materials in saturated/unsaturated conditions

Cyclic triaxial tests on the rock materials of Dam A were carried out in saturated/unsaturated conditions.

The rock materials of Dam A were dacites.

The rock materials were compacted in a relative density of $Dr = 85\%$.

The lateral stress of σ_r in a saturated condition was decided based on the normal minor principal stress in the upstream rock zone of a 100-meter-high rockfill dam model during impounding period. The lateral stress of σ_r in an unsaturated condition was decided based on the normal minor principal stress in the downstream rock zone. The consolidation stress ratio of σ_1/σ_3 was set at 2.0.

Figure 3 shows the cumulative strain in both saturated and unsaturated conditions. Very small strain is generated in unsaturated conditions in comparison with that in saturated conditions.

3 SEISMIC DEFORMATION ANALYSIS OF AN EARTH CORE ROCKFILL DAM (ECRD)

Based on the test results in Chapter 2, we decided the dynamic strength properties of the dam body materials taking into account the confining pressure and saturated/unsaturated conditions during the impounding period, and performed cumulative damage analysis. Effects of these conditions on the earthquake-induced settlement of an ECRD were investigated.

4 OUTLINE OF ANALYTICAL PROCEDURE

In this study, the static stress distribution within a dam body was calculated by static analyses including embanking and impounding processes. Based on this as the initial stress, a dynamic analysis was conducted to evaluate the effect of an earthquake on the dam (Inomata, 2005). As for the embankment analysis, the nonlinear elasticity analysis based on the Duncan-Chang model was employed. The stress at impounding was calculated taking into consideration the effect of the seepage force on the core zone and of the buoyancy on a submerged section. In the dynamic analysis, the complex response analysis based on the equivalent linearization method was adopted, where only the dam body was modeled and the benthic boundary was fixed. Therefore, energy dissipation in the foundation was considered with a dissipation damping

ratio. CDTA is based on the concept that a permanent displacement caused by an earthquake can be attributed to residual strain that occurs under the influence of cyclic loading.

4.1 Analytical conditions

The analytical model, an ECRD with a height of 100 m is shown in Figure 4. The water level was determined to be 92 m on the assumption of a normal water level for a common rockfill dam in Japan. The physical properties used in the dynamic analysis based on the equivalent linearization method are shown in Figure 5.

Table 1 summarizes equations concerning the cumulative strain properties, which were formulated from the dynamic strength tests for each material.

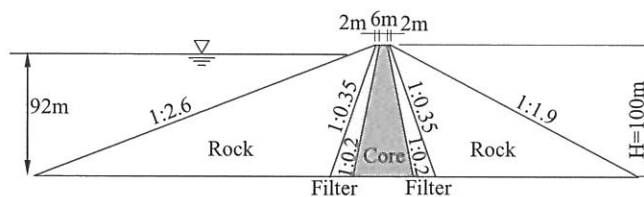


Figure 4. Analytical model.

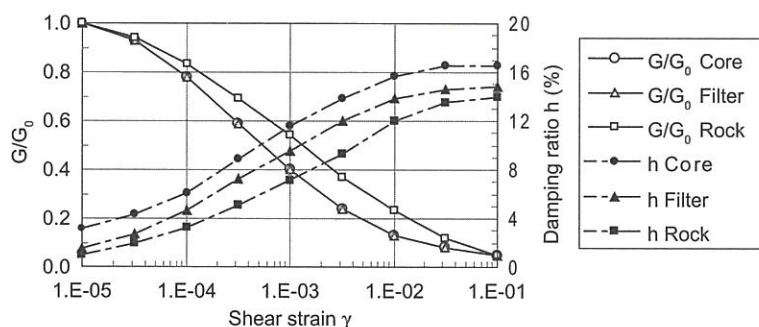


Figure 5. Relationship between G/G_0 , h and γ .

Table 1. Cumulative strain properties.

Property	Zone	Equation
T	Core	$SR_d = 0.43\epsilon^{0.50} \times Nc^{-0.33} + 0.16$
	Filter	$SR_d = 0.59\epsilon^{0.47} \times Nc^{-0.33} + 0.16$
	Rock (i)	$\sigma'_m > 0.196 \text{ MPa}$ $SR_d = 0.65\epsilon^{0.50} \times Nc^{(-0.34\epsilon^{0.01})} + 0.20$
	Rock (ii)	$0.098 < \sigma'_m \leq 0.196 \text{ MPa}$ $SR_d = 1.05\epsilon^{0.70} \times Nc^{(-0.25\epsilon^{0.01})} + 0.25$
	Rock (iii)	$\sigma'_m \leq 0.098 \text{ MPa}$ $SR_d = 2.00\epsilon^{0.80} \times Nc^{(-0.28\epsilon^{0.01})} + 0.26$
A	Core	Unsaturated $SR_d = 2.15\epsilon^{0.90} \times Nc^{(-0.51\epsilon^{0.08})} + 0.19\epsilon^{0.25}$
		Saturated $SR_d = 0.23\epsilon^{0.60} \times Nc^{(-0.40\epsilon^{0.33})} + 0.19\epsilon^{0.21}$
	Filter	Unsaturated $SR_d = 0.44\epsilon^{0.07} \times Nc^{-0.17} + 0.06\epsilon^{1.46}$
		Saturated $SR_d = 0.22\epsilon^{0.87} \times Nc^{(-0.45\epsilon^{0.09})} + 0.21\epsilon^{0.15}$
	Rock	Unsaturated $SR_d = 0.47\epsilon^{0.07} \times Nc^{-0.17} + 0.37\epsilon^{1.46}$
		Saturated $SR_d = 0.57\epsilon^{2.01} \times Nc^{(-0.96\epsilon^{0.17})} + 0.38\epsilon^{0.03}$

* SR_d : Cyclic shear stress ratio, Nc : Number of cycles, ϵ : Axial strain (%).

earthquake
ng.

water level
non rockfill
equivalent

which were

In the CDTA, we used Property T in Table 1 to examine the effects of confining pressure and Property A in Table 1 to examine the effects of the saturated/unsaturated conditions.

The results of the undrained cyclic triaxial tests carried out by Yonesaki *et al.* (Yonesaki, 2000) on the core materials and sand-gravel filter materials of ECRD were employed for the core materials and filter materials of Property T. As shown in Chapter 2, on the rock materials, Matsumoto *et al.* (Matsumoto, 1991) performed undrained cyclic triaxial tests, where various values of confining pressures were examined for the ECRD rock materials. Among these values, the effective mean stresses of $\sigma'_m = 0.098, 0.196$ and 0.588 MPa were employed. Figure 6 illustrates the cumulative strain properties of Property T.

Property A was derived from the results of cyclic triaxial tests that were carried out on the construction materials used for Dam A. However, no cyclic triaxial tests were performed in unsaturated condition on the filter materials of Dam A. Thus, the cumulative strain properties of the filter materials in saturated condition were estimated from (1) the cumulative strain properties of the filter materials in unsaturated condition and (2) the cumulative strain properties of the rock materials in saturated/unsaturated condition. Figure 7 shows the cumulative strain properties of Property A.

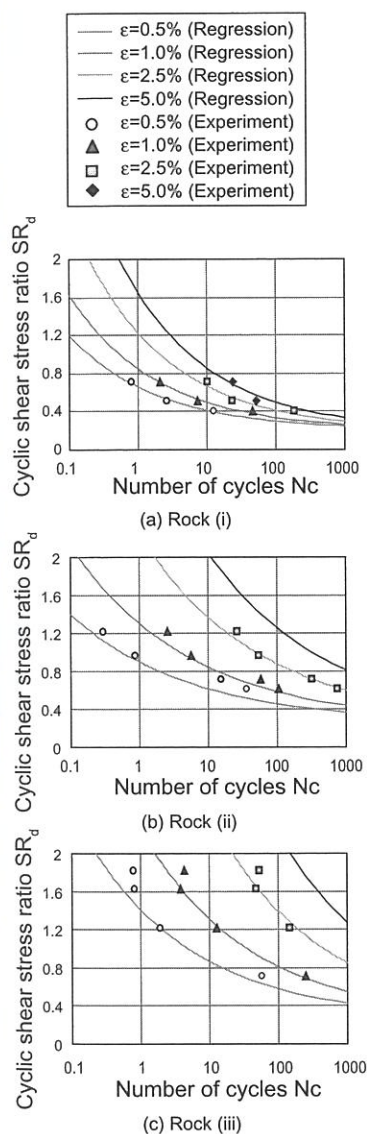


Figure 6. Cumulative strain properties of Property T (rock materials).

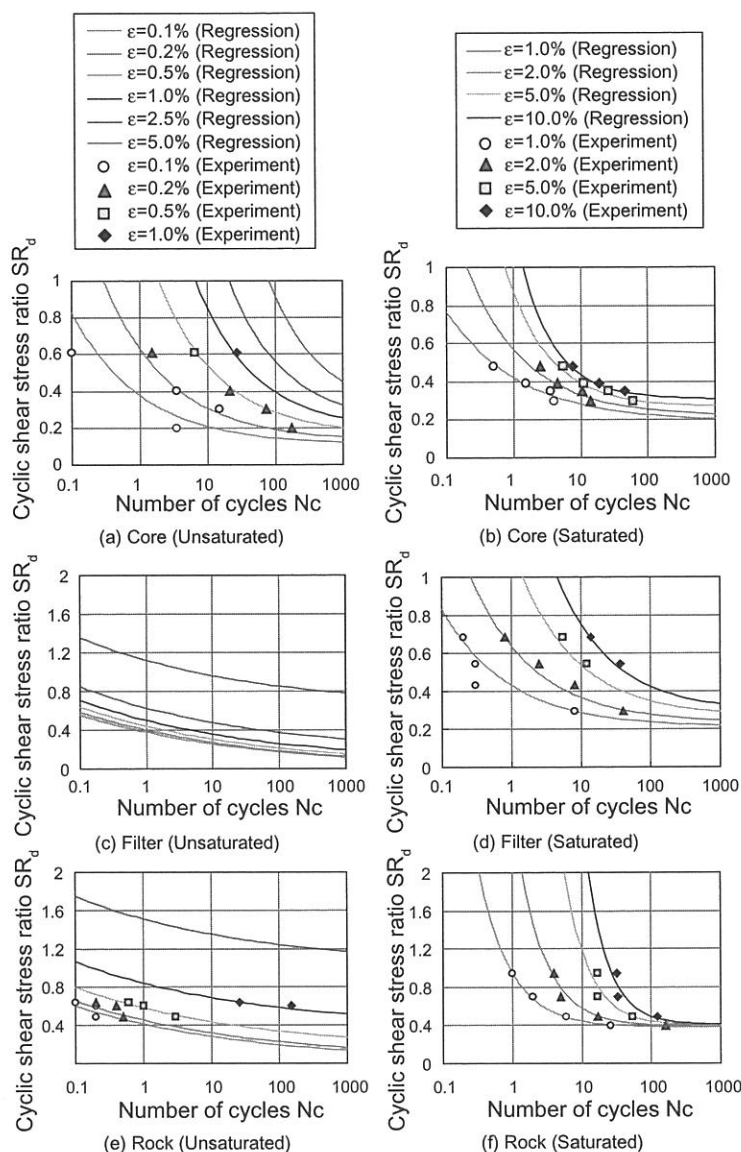


Figure 7. Cumulative strain properties of Property A.

The input earthquake motions were prepared based on the observed waves at dam foundations during the 1995 South Hyogo Prefecture Earthquake, namely the Hitokura Dam Wave, the Minoogawa Dam Wave, and the Gongen Dam Wave. The maximum horizontal accelerations of three waveforms were adjusted as 7.20 m/s^2 simply by increasing those amplitudes in proportion to the observed maximum accelerations. Figure 8 shows the time histories of the horizontal accelerations of the three input waves. Figure 9 illustrates the acceleration response spectra of these three waveforms.

Analytical cases are listed in Table 2. The analytical cases were intended to evaluate effects on the CDTA of dynamic strength properties considering effective confining pressure and saturated/unsaturated conditions.

Cases 1 and 2 show examinations of the effects of the mean effective stress during the impounding period. In Case 1, the value of $\sigma'_m = 0.588 \text{ MPa}$ for Property T was applied to the entire rock zone, and in Case 2 cumulative strain properties of the rock zone were assigned in response to the initial mean effective stress. In Cases 3 and 4, the effects of saturated/unsaturated conditions are examined. Case 3 deals with Property A only in a saturation condition whereas Case 4 deals with physical properties in both saturated/unsaturated conditions.

4.2 Analytical results

The analytical results are summarized in Table 3.

The maximum settlement in the CDTA increases in an ascending order of: Hitokura Dam.

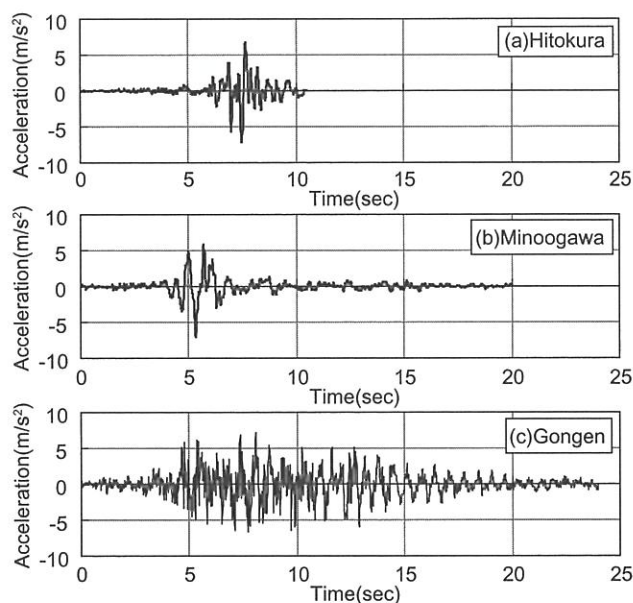


Figure 8. Time histories of accelerations of the input motions (upstream-downstream direction).

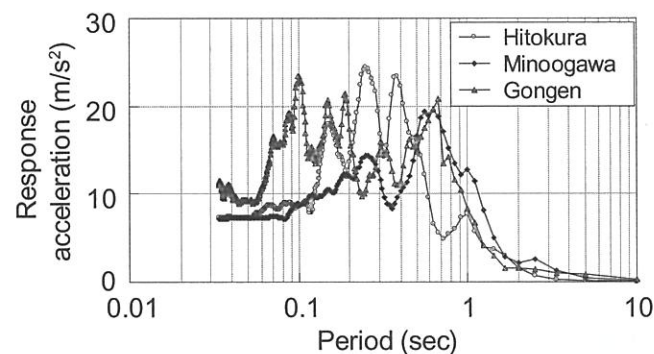


Figure 9. Acceleration response spectra (upstream-downstream direction).

Table 2. Analytical cases.

Case	Input waveform	Maximum acceleration m/s ²	Dynamic strength	How to assign the dynamic strength			Remarks
				Core	Filter	Rock	
1-1	Hitokura	7.20	T	Property T		Rock (i) was applied to the entire rock zone	Effects of mean effective stress
1-2	Minoogawa						
1-3	Gongen						
2-1	Hitokura	7.20	T	Property T		Assigned in response to the initial mean effective stress	
2-2	Minoogawa						
2-3	Gongen						
3-1	Hitokura	7.20	A			Deals with Property A only in a saturated state	Effects of saturated/unsaturated
3-2	Minoogawa						
3-3	Gongen	states					
4-1	Hitokura	7.20	A			Deals with Property A in both saturated/unsaturated conditions	
4-2	Minoogawa						
4-3	Gongen						

Table 3. Analytical results.

Case	Natural period		Maximum acceleration at crest		Cumulative damage analysis*1)					
	Initial rigidity (s)	Convergent rigidity (s)	horizontal (m/s ²)	vertical (m/s ²)	Maximum settlement			Maximum horizontal displacement*2)		
					U (cm)	C (cm)	D (cm)	U (cm)	C (cm)	D (cm)
1-1	0.572	0.838	13.51	11.68	75.6	72.4	36.7	-107.7	-38.0	-13.9
1-2		0.908	13.94	10.03	142.3	139.1	98.6	-44.7	-47.4	-21.0
1-3		0.851	10.57	6.36	226.7	212.8	123.4	-275.4	-101.1	-49.9
2-1	0.572	0.838	13.51	11.68	50.8	55.4	30.5	-35.0	-16.0	-10.4
2-2		0.908	13.94	10.03	109.1	112.8	85.5	-47.3	-14.7	-12.0
2-3		0.851	10.57	6.36	157.6	161.7	105.4	-76.9	-31.3	-24.4
3-1	0.572	0.838	13.51	11.68	117.4	122.3	86.8	-68.7	-31.8	-27.3
3-2		0.908	13.94	10.03	189.3	193.8	159.6	-75.0	-49.4	-48.0
3-3		0.851	10.57	6.36	368.3	377.5	243.4	-169.8	-120.5	-107.7
4-1	0.572	0.838	13.51	11.68	100.6	96.6	69.6	-69.7	-44.9	-38.6
4-2		0.908	13.94	10.03	171.4	171.0	145.8	-75.8	-57.6	-56.1
4-3		0.851	10.57	6.36	295.0	273.2	190.4	-173.0	-148.7	-142.2

*1) C: 10 m section at crest, U: entire upstream slope excluding the crest, D: entire downstream slope excluding the crest.

*2) Positive values are given to the downstream side.

Wave, Minoogawa Dam Wave, and Gongen Dam Wave in all cases.

The maximum horizontal displacement in the CDTA was always on the upstream side, increasing in an ascending order of: Hitokura Dam Wave, Minoogawa Dam Wave, and Gongen Dam Wave in all cases except for the displacement at the crest in Case 2.

We then focused on the analytical results of the Gongen Dam Wave, which generated the largest settlement and horizontal displacement, to examine the effects of initial mean effective stress and saturated/unsaturated conditions on the dam body deformation. Figures 10 through 13 show the distributions of the dam body settlement and horizontal displacement under each comparative condition.

4.2.1 Effects of confining pressure

The horizontal displacement as well as the settlement of a dam body surface tends to decrease with the consideration of effects of confining pressure on dynamic strength. The degree of decrease in deformation is large on the upstream side.

According to the vertical distribution of settlements in the bottom of Figure 10, in large confining pressure areas, the settlements for Case 1 and Case 2 are almost same. But, the difference between Case 1 and Case 2 becomes large near the surface where the confining pressure is small. Particularly, because of decrease in effective stress due to impounding, the difference in settlement is large near the surface of an upstream rock zone where the confining pressure is small.

Regarding the vertical distribution of horizontal displacement illustrated in the bottom of Figure 11, the horizontal displacements in both cases are almost same at large confining pressure area, but difference of the horizontal displacements is large near the surface in small confining pressure area.

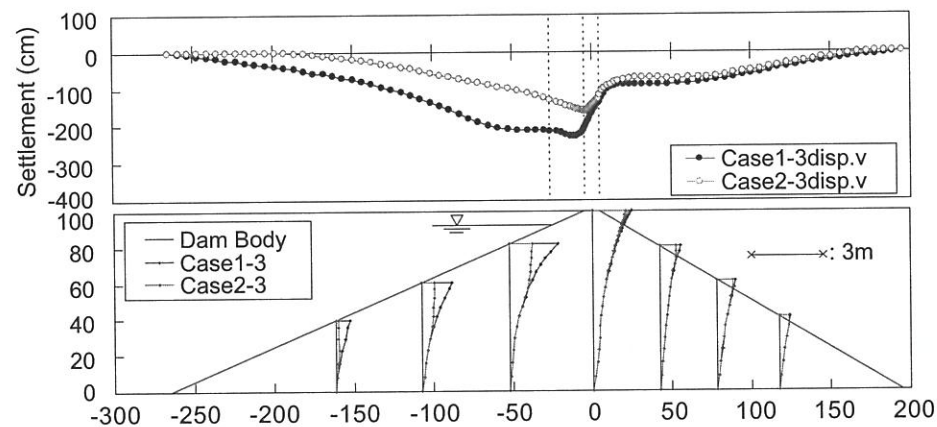


Figure 10. Effects of mean effective stress (confining pressure) on settlement. (Top: settlement of dam body surface, Bottom: vertical distribution of settlement).

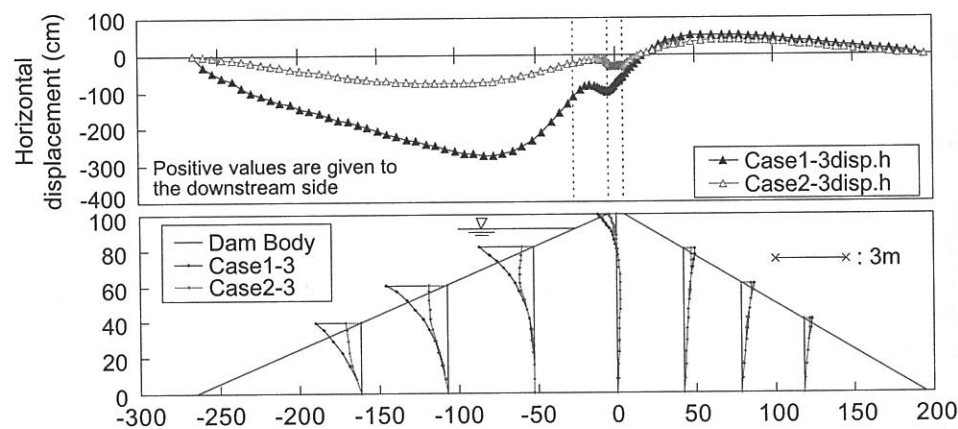


Figure 11. Effects of mean effective stress (confining pressure) on horizontal displacement. (Top: horizontal displacement of dam body surface, Bottom: vertical distribution of horizontal displacement).

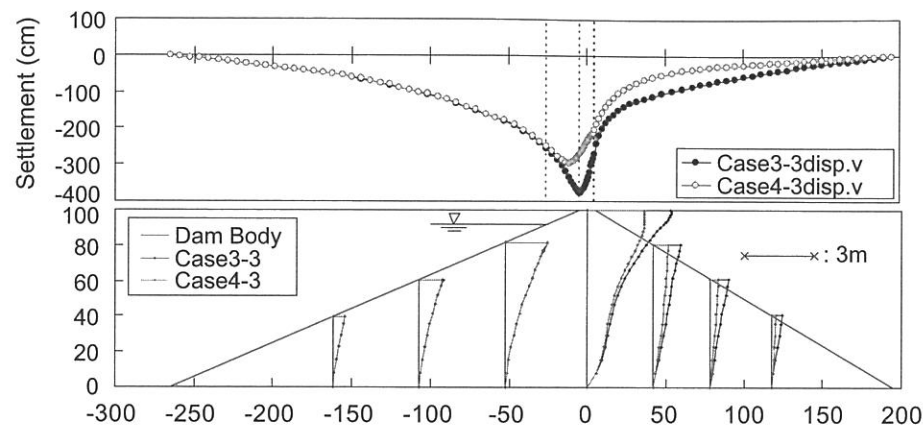


Figure 12. Effects of saturated/unsaturated conditions on settlement. (Top: settlement of dam body surface, Bottom: vertical distribution of settlement).

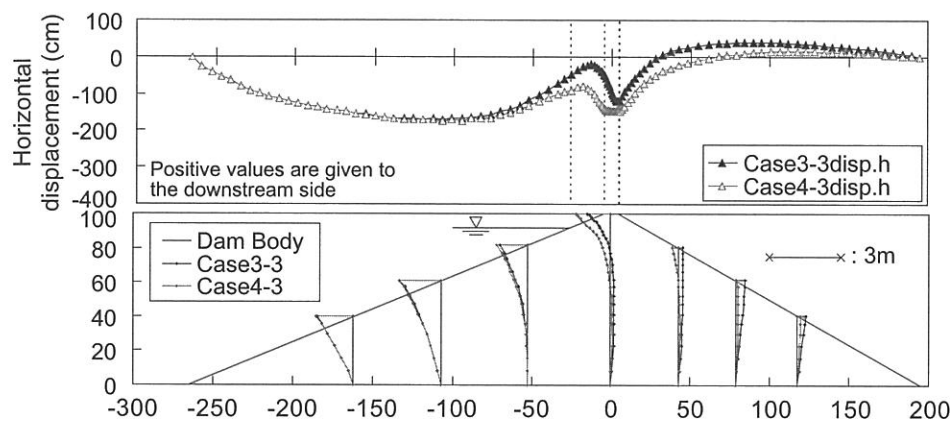


Figure 13. Effects of saturated/unsaturated conditions on horizontal displacement. (Top: horizontal displacement of dam body surface, Bottom: vertical distribution of horizontal displacement).

4.2.2 Effects of saturated/unsaturated conditions

Little difference was seen between Case 3 and Case 4 in horizontal displacement as well as settlement of dam body surface in upstream side below the reservoir water level. Regarding the unsaturated area above a reservoir water level, as the vertical distribution of horizontal displacement in the bottom of Figure 13 indicates, the distribution of horizontal displacement in Case 4, which considers an unsaturated condition, appears to be affected by the deformation in downstream rock zone to downstream direction. Settlement in unsaturated area in Case 4 is smaller than that in Case 3.

In the bottom of Figure 12, a comparison of the settlements in the saturated areas between Case 3 and Case 4 reveals that they are almost same. In the unsaturated area (above El. 92 m) and the downstream zone, however, the settlement in Case 4, where the unsaturated area was taken into account, is smaller than that of Case 3.

5 CONCLUSIONS

1. We carried out cyclic triaxial tests to evaluate the effects of mean effective stress (confining pressure) and saturated/unsaturated conditions on the dynamic strength properties of rockfill dam materials. As a result, we found that the dynamic strength of dam materials becomes large with a decrease in the mean effective stress, and that the dynamic strength in an unsaturated condition is large in comparison with that in a saturated condition.

2. We used the dynamic strength properties obtained in Chapter 2 to the CDTA of a 100-meter-high ECRD model. As a result, we found that the initial mean effective stress and saturated/unsaturated conditions had significant effects on the settlement and displacement.

REFERENCES

- East Japan Railway Company (JR East Co.), 2006, Report of Technical Specialist Committee on the Shinano River Power Plant Restoration Works, pp. 69–101. (in Japanese).
- Inomata, J., Nagayama, I. et al., 2005, Technical Report on Seismic Performance Evaluation of Dams against Large Earthquakes, in Journal of National Institute for Land and Infrastructure Management, No. 244/ Technical Memorandum of PWRI, No. 3965. (in Japanese).
- Japan Dam Engineering Center (JDEC), 2001, Sectional Meeting Report on Rationalization of Embankment Dam Design. (in Japanese).
- Matsumoto, N., Yasuda, N., Okubo, M., & Yoshioka, R. 1991, Monotonic Loading Tests and Cyclic Loading Tests for Rock Materials, Technical Memorandum of PWRI, No. 2996. (in Japanese).
- River Bureau, Ministry of Land, Infrastructure, Transport and Tourism (MLIT), 2005, Guidelines for Seismic Performance Evaluation of Dams During Large Earthquakes (Draft). (in Japanese).
- Satoh H. & Yamaguchi Y. 2007, Dynamic strength of core materials with compaction degree, Engineering for Dams, No. 252, pp. 42–53. (in Japanese).
- Yonesaki, F., Sato, N., & Someya, T. 2000, Study on Seismic Design for Structures—Seismic Diagnosis for the Tokuyama Dam against Level 2 Ground Motions, Research Institute, Water Resources Development Public Corporation, No. 99213, 2000. (in Japanese).